Breaking the "one nucleus, one whole genome" rule: *Neurospora crassa* separates its haploid chromosomes into different nuclei

Jinyi Tan[1,3¶], Yan Xu[2 ¶], Piao Yang[4], Shuai Huang[4], Monika Fischer[1], Yuelin Zhang[2] and Xin Li[1,3*]

[1] Michael Smith Laboratories, University of British Columbia, Vancouver BC V6T 1Z4, Canada

[2] Key Laboratory of Bio-resource and Eco-environment of Ministry of Education, the College of Life Sciences, Sichuan University, Chengdu, 610064, Sichuan, China

[3] Department of Botany, University of British Columbia, Vancouver BC V6T 1Z4, Canada

[4] Department of Molecular Genetics, Ohio State University, Columbus, OH43210, USA

[¶] These authors contributed equally to the study.

* For correspondence: Xin Li; Email: xinli@msl.ubc.ca

Abstract

The nucleus is a defining feature of eukaryotic cells, compartmentalizing the genome to enable precise regulation of diverse cellular processes. The long-standing paradigm in textbooks states that each nucleus carries at least a complete haploid genome —the "one nucleus, one whole genome" rule. A striking exception was recently uncovered: in two sclerotia-forming plant pathogenic fungi in the Sclerotiniaceae family, *Sclerotinia sclerotiorum* and *Botrytis cinerea*, haploid chromosomes are irregularly distributed across multiple nuclei. However, whether such phenomenon occurs in other eukaryotes, particularly in non-pathogenic fungi, is unclear. Through a literature survey, we identified many fungi that can potentially also separate their haploid chromosomes across different nuclei. Interestingly, *Neurospora crassa*, a foundational fungal genetics model, came out as a candidate. Its conidia, typically containing two or three nuclei, were believed to harbor a complete haploid genome within each nucleus. However, using approaches including chromosome counting, flow cytometry, and fluorescence in situ hybridization, we found that haploid chromosomes in *N. crassa* can be unevenly distributed among multiple nuclei. These findings challenge longstanding assumptions in fungal genetics and provide new directions for investigating genome organization. Our results indicate that the organisms violating the "one nucleus, one whole genome" rule are beyond sclerotia-forming pathogenic fungi. Since over 90% of fungi have not even been described, we propose that many more of them may likewise partition their genomes non-uniformly across nuclei, a process that could facilitate their adaptation and evolution.

37 **Introduction**

38 A defining feature of eukaryotes is the presence of nuclei, which compartmentalize genetic
39 material and orchestrate gene expression. It has been long held that each nucleus contains at least
40 one full set of chromosomes required for proper genomic function and cellular development – an
41 assumption referred to as the "one nucleus, one whole genome" rule. However, our recent study
42 challenges this long-standing principle. Using chromosomal counting, fluorescence in situ
43 hybridization (FISH), flow cytometry-based DNA quantification, and single-nucleus polymerase
44 chain reaction (PCR) analyses, we uncovered that in two plant pathogenic fungi belonging to the
45 Sclerotiniaceae family –*Sclerotinia sclerotiorum* and *Botrytis cinerea* – haploid chromosomes
46 are distributed among different nuclei (1).

47 Such finding raises the next question of how widespread this unconventional mode of
48 chromosomal organization is. Both *S. sclerotiorum* and *B. cinerea* produce bi- or multinucleate
49 spores. Interestingly, they also generate uninucleate spermatia that are not viable, likely due to
50 the incomplete chromosome sets within (2,3). To explore whether similar chromosomal
51 partitioning pattern might be more widespread, we undertook an extensive literature survey
52 focusing on fungal species reported to produce bi- or multinucleate spores along with a high
53 frequency of nonviable uninucleate cells (4). These species were considered likely candidates
54 that may also be breaking the "one nucleus, one whole genome" rule. Interestingly, *Neurospora*
55 *crassa* came out as a prime candidate. Although it can produce viable uninuclear microconidia,
56 more than 60% are nonviable, possibly due to the absence of a complete chromosome
57 complement (5,6).

58 *N. crassa* is a non-pathogenic ascomycete that has long served as a classical model organism in
59 fungal genetics and molecular biology, contributing to landmark discoveries such as the "one

60 gene, one enzyme" hypothesis (7,8). Owing to its well-characterized genetics and ease of
61 manipulation, *N. crassa* was almost the first filamentous fungus to have its genome fully
62 sequenced, establishing it as a preferred model for genome-wide functional studies and for
63 numerous discoveries related to chromosomal behavior and gene regulation (9–11). Its genome,
64 approximately 40 Mb in size, is organized into seven linkage groups as determined through
65 pulsed-field gel electrophoresis (PFGE) and whole-genome sequencing and assembly (9,10,12).
66 In this short report, through chromosome counting, flow cytometry and fluorescence in situ
67 hybridization (FISH) analyses, we show that *N. crassa* can partition its haploid genome across
68 multiple nuclei, thereby extending the scope of breaking the "one nucleus, one whole genome"
69 rule beyond the Sclerotiniaceae family.

70

71 **Results**

72 *N. crassa* produces abundant asexual spores, known as conidia, which are typically
73 multinucleate. When we grew *N. crassa* on potato dextrose agar (PDA), majority of fresh conidia
74 contain 2 to 3 nuclei (Figure 1A), whereas conidia from older cultures show an obvious increase
75 in nuclear number, with a higher proportion containing more than three nuclei (Figure 1B and
76 C). This indicates that genomes within the conidia are not predefined; rather, they can undergo
77 endoreduplication through time and become more variable. To quantify the DNA amount in each
78 nucleus, we employed flow cytometry through fluorescence-activated cell sorting (FACS) using
79 purified nuclei from fresh mycelia. Haploid and diploid *Saccharomyces cerevisiae* strains
80 BY4741 and BY4743, and the filamentous plant pathogen *S. sclerotiorum* were used as controls.
81 Based on the relative fluorescence intensity (RFI) of nuclei (Figure 2A and B), each nucleus

contained about a quarter of its full haploid genome, suggesting that each nucleus within *N. crassa* mycelia harbors only parts of its full genome (Figure 2C).

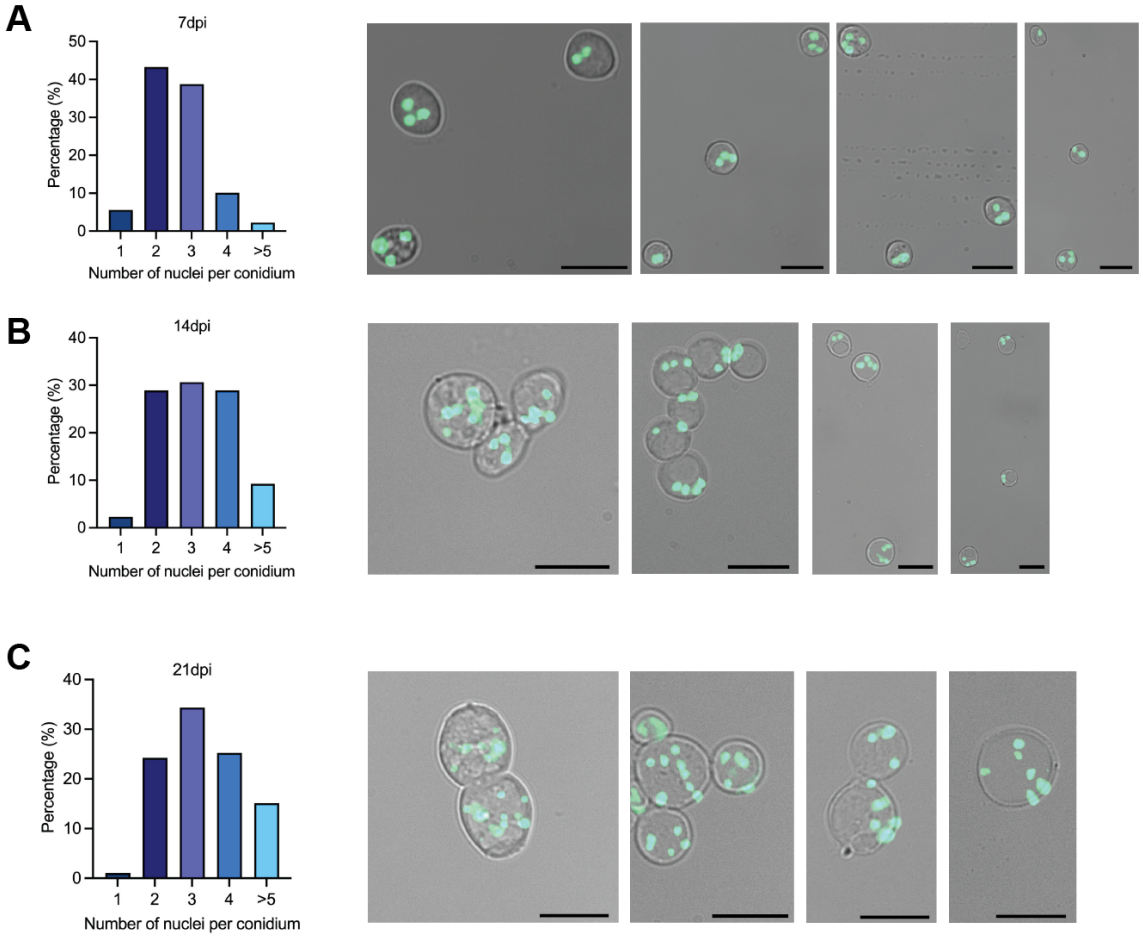

Figure 1. *N. crassa* conidia have multiple nuclei, with nuclear number increasing as culture ages.
(A) Quantification of conidial nuclei number in fresh culture at 7 days post-inoculation on PDA (7 dpi) (left). Representative fluorescence microscopy images of conidial nuclei in the hH1-sGFP strain are shown (right). Scale bar, 10 µm.
(B) Quantification of conidial nuclei number under the same condition at 14 dpi (left). Representative fluorescence microscopy images of conidial nuclei in the hH1-sGFP strain are shown (right). Scale bar, 10 µm.
(C) Quantification of conidial nuclei number under the same condition at 21 dpi (left). Representative fluorescence microscopy images of conidial nuclei in the hH1-sGFP strain are shown (right). Scale bar, 10 µm.

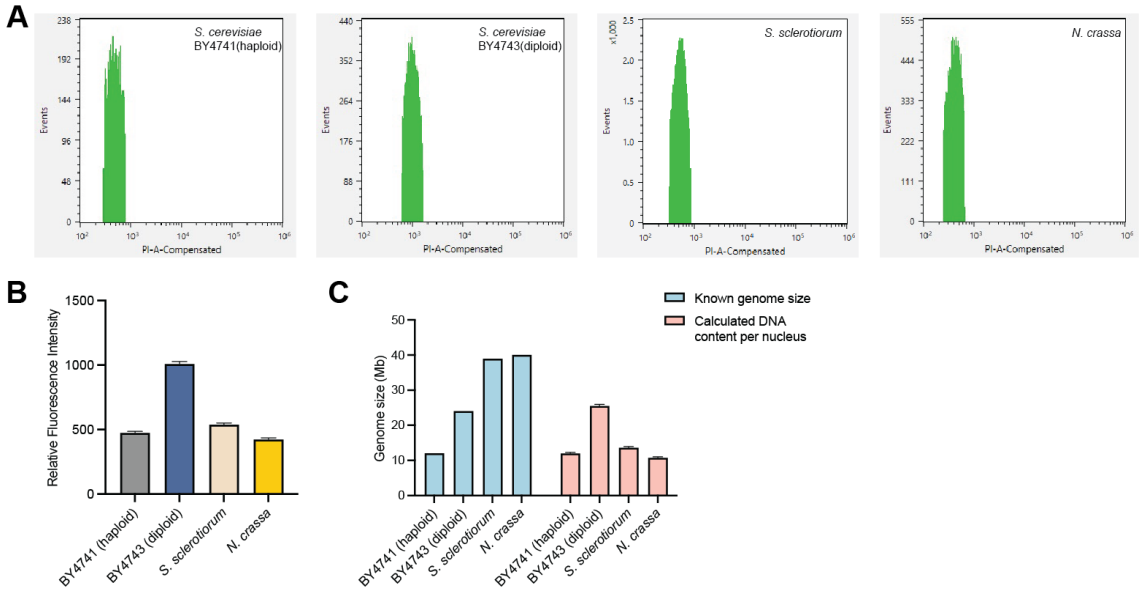

Figure 2. On average, each nucleus of *N. crassa* contains a portion of its haploid genome.
(A) Nuclei sorting by FACS. The isolated nuclei from *Saccharomyces cerevisiae* BY4741 (haploid), BY4743 (diploid), *S. sclerotiorum* and *N. crassa* mycelia were flowed into the Sony MA900 cell sorter. The selected events were plotted with the number of events against the PI fluorescence intensity.
(B) Propidium iodide (PI) fluorescence intensity of sorted purified nuclei from *S. cerevisiae* BY4741, BY4743, *S. sclerotiorum* and *N. crassa* mycelia. The PI fluorescence intensity values were calculated based on the mean fluorescence intensity of each individual well. Error bars indicate the standard deviation of the values from 15 wells.
(C) Calculated DNA content per nucleus in *S. cerevisiae* BY4741, BY4743, *S. sclerotiorum* and *N. crassa*. The known genome sizes of these strains are 12, 24, 38.9 and 40 Mb, respectively. The DNA content in each nucleus was calculated by multiplying the genome size of the haploid yeast strain BY4741 by the fold-change values derived from Fig 2B. Error bars indicate the standard deviation (n = 15).

We then counted chromosomes inside the protoplasts isolated directly from the conidia. As observed in *S. sclerotiorum*, where most ascospores harbor approximately 16 chromosomes (1), the largest percentage of *N. crassa* conidia contains around seven chromosomes (Figure 3A, B and E). However, substantial proportions harbor more than seven chromosomes, with counts reaching up to 22. These observations suggest that aneuploidy may be more common in *N. crassa* conidia, and that conidia containing equal to or more than 14 chromosomes could have arisen through endoreduplication (Figure 3D and E). Live-cell observation of the *N. crassa* strain carrying the hH1-sGFP (green fluorescence protein fused with histone H1) transgene with confocal fluorescence microscopy further confirmed substantial variation in chromosome

number among nuclei. Although precise chromosome counts are difficult to determine using hH1-sGFP fusion strains, the observed numbers were largely fewer than seven (see S1 Movie, showing division of a nucleus with about two chromosomes, and S2 Movie, showing division of a nucleus with approximately four chromosomes). Together, these data support that most viable conidia are haploid and can separate their haploid genome into different nuclei.

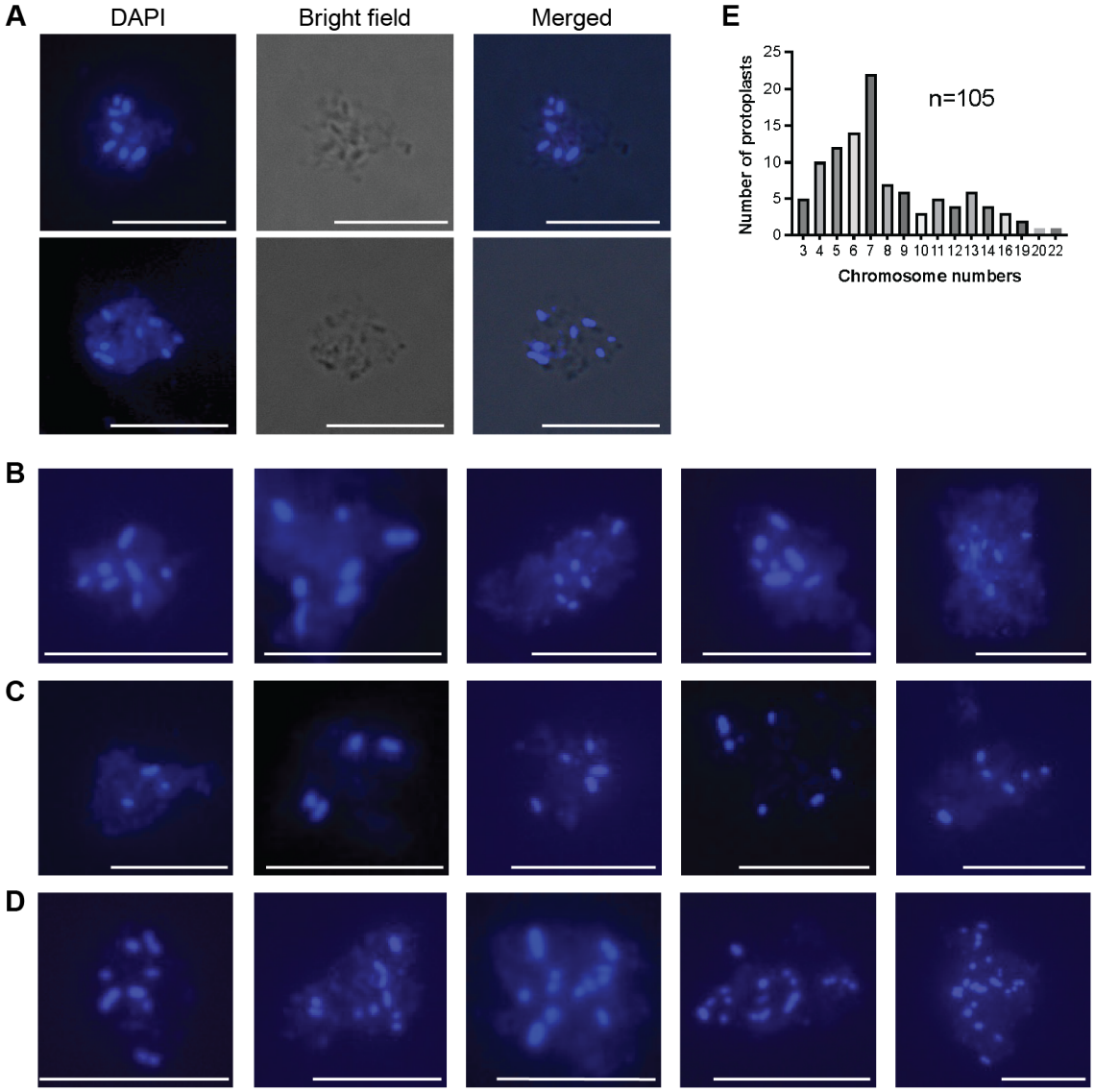

Figure 3. Chromosome counts from *N. crassa* conidial protoplasts.
(A) DAPI stained chromosomes inside two representative conidial protoplasts. Scale bar, 10 µm.
(B) DAPI-stained conidial protoplasts showing seven chromosomes. Scale bar, 10 µm.
(C) DAPI-stained conidial protoplasts showing fewer than seven chromosomes. Scale bar, 10 µm.

126 **(D)** DAPI-stained conidial protoplasts showing more than seven chromosomes. Scale bar, 10 µm.
127 **(E)** Distribution histogram of chromosome counts from a total of 105 protoplasts of *N. crassa* conidia.
128

129 Lastly, to corroborate our observations, we performed fluorescence in situ hybridization (FISH)
130 using linkage group I (LG I)- and linkage group IV (LG IV)- specific probes (Figure 4A). When
131 these probes were applied individually, hybridization signals were consistently detected in only
132 one nucleus per conidium (Figure 4B and C). Importantly, probe signals were never detected
133 simultaneously in multiple nuclei within the same conidium (Figure 4B, C and D). As a control,
134 a telomere repeat probe that is present in all linkage groups yielded signals mostly in all nuclei
135 (Figure 4A), confirming that probe accessibility was not limiting (Figure 4B, C and D).
136 Interestingly, the intensity of the fluorescence signals from the telomere repeat probe can be
137 drastically different among nuclei within the same cell, likely reflecting the different number of
138 chromosomes within (Figure 4B and C). The intensity of the signals also seems to correlate with
139 the size of the nuclei. A similar trend was observed in live-cell imaging using the hH1-sGFP
140 strain, where nuclei containing fewer chromosomes appeared smaller than those harboring more
141 chromosomes. Thus, haploid chromosomes in *N. crassa* can partition unevenly in these bi- or tri-
142 nuclear conidia.

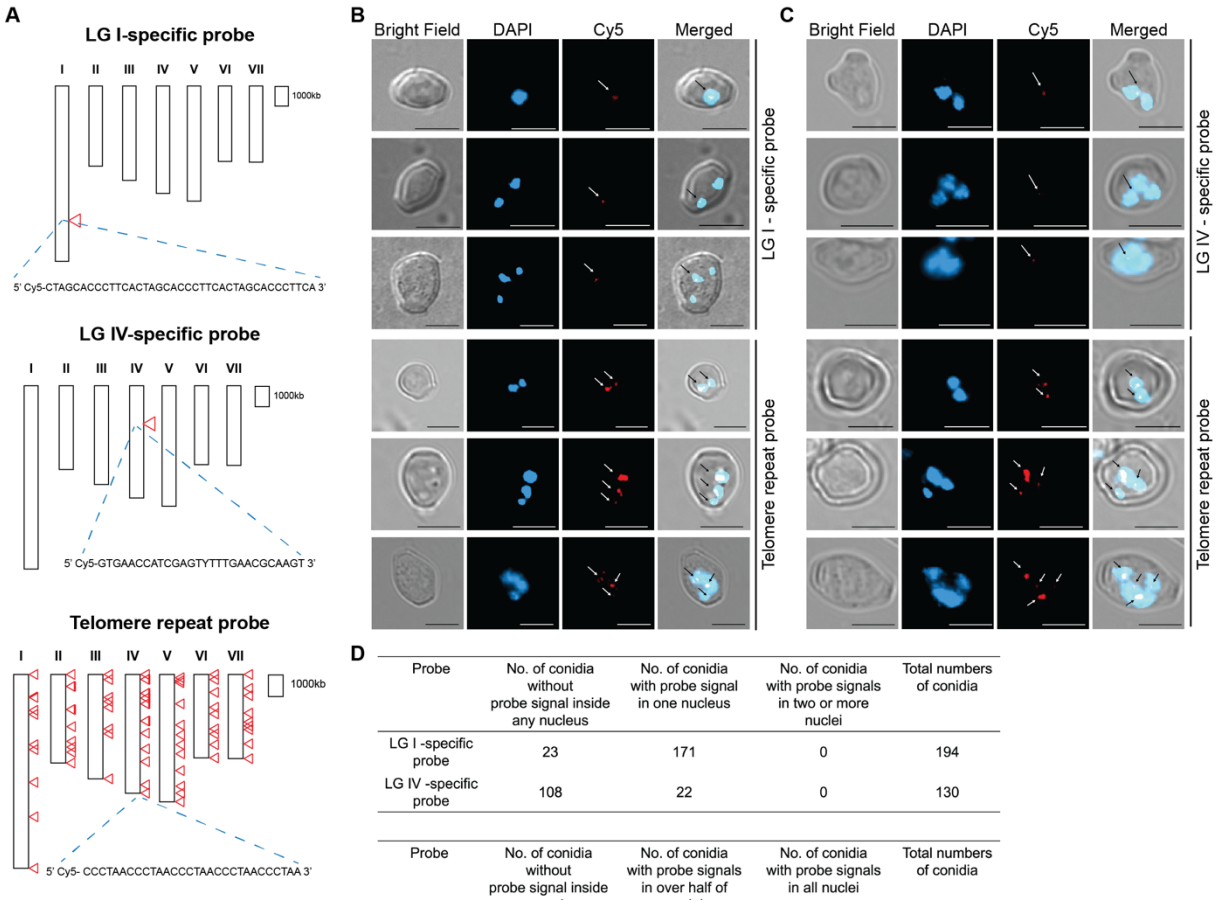

D

Probe	No. of conidia without probe signal inside any nucleus	No. of conidia with probe signal in one nucleus	No. of conidia with probe signals in two or more nuclei	Total numbers of conidia
LG I -specific probe	23	171	0	194
LG IV -specific probe	108	22	0	130

Probe	No. of conidia without probe signal inside any nucleus	No. of conidia with probe signals in over half of nuclei	No. of conidia with probe signals in all nuclei	Total numbers of conidia
Telomere repeat probe	15	29	79	123

Figure 4. A *N. crassa* conidium can separate its haploid chromosomes into one, two, or three nuclei.
(A) The hybridization sites of the LG I-specific (top), LG IV-specific (middle) and telomere repeat (bottom) probes on the *N. crassa* chromosomes as indicated by red triangles.
(B) FISH signals of LG I-specific (top) and non-specific (bottom) probes in representative conidia. Blue and red signals are from DAPI-stained nuclei and hybridized fluorescent probe, respectively. The hybridized Cy5 probe signals are pointed out by arrows. Scale bars, 5 µm.
(C) FISH signals of LG IV-specific (top) and non-specific (bottom) probes in representative conidia. Blue and red signals are from DAPI-stained nuclei and hybridized fluorescent probe, respectively. The hybridized Cy5 probe signals are pointed out by arrows. Scale bars, 5 µm.
(D) Summary of FISH results for LG I-, LG IV-specific and telomere repeat probes. Among conidia with a single LG I-specific signal, 6% were uninucleate, 48% contained two nuclei, 35% contained three nuclei, and 11% contained four or more nuclei. For conidia with a single LG IV-specific signal, 22 contained two nuclei and 5 contained three nuclei. The lower number of conidia exhibiting a LG IV-specific probe signal is likely due to reduced probe hybridization efficiency or limited accessibility caused by the presence of a degenerate nucleotide in the probe.

160 **Discussion**

161 Our data here support the conclusion that *N. crassa* conidia can partition their haploid
162 chromosomes among different nuclei, expanding the range of species in which genome
163 partitioning across nuclei has been observed. This feature will offer a major practical advantage.
164 For gene replacement experiments to knock out or modify target genes, fresh conidia are already
165 being used, skipping the step of uninucleate microconidia purification (13). The same is true for
166 mutagenesis in forward genetic analyses (14). Just as with *S. sclerotiorum*, binucleate ascospores
167 or multinuclear conidia of *N. crassa* can be used with UV or chemical mutagens to generate pure
168 haploid mutants (15).

169 Interestingly, uninucleate *N. crassa* microconidia exhibit a low germination rate of about 10-30%
170 (6,16), whereas uninucleate spermatia cells in *S. sclerotiorum* and *B. cinerea* are completely
171 nonviable likely due to the incomplete genomes within (2,3). We believe the reason why a small
172 fraction of the uninucleate microconidia is viable in *N. crassa* is probably due to its low haploid
173 chromosome number. Its seven chromosomes may occasionally be packed into just one nucleus,
174 allowing the spore to be viable. As for *S. sclerotiorum* and *B. cinerea*, 16 or 18 chromosomes are
175 seemingly almost impossible to be packed simultaneously into a single nucleus during nuclear
176 division.

177 The chromosomal and nuclear states in *N. crassa* conidia appear to be more complex than those
178 of haploid *S. sclerotiorum* ascospores. Based on our chromosome counting results, although the
179 largest percentage of *N. crassa* conidia have seven chromosomes, a substantial fraction contains
180 more. Together with the observed increase in number of nuclei inside the conidia through time,
181 these data suggest that some *N. crassa* conidia may be aneuploid, while others may contain two
182 or more chromosome sets as a result of mitotic divisions occurring after initial conidial

183 formation. Similar pattern could exist with multinuclear conidia of other fungi, such as *B.*
184 *cinerea*. Such genomic flexibility in conidia may help the survival and quick adaptation of the
185 organism.

186 In summary, our findings in *N. crassa* suggest that dividing haploid chromosomes across
187 multiple nuclei may be more widespread than previously recognized. It is not restricted to
188 sclerotia-forming plant fungal pathogens of the Sclerotiniaceae family. Other Ascomycetes and
189 Basidiomycetes with known bi- or multi-nucleate ascospores and basidiospores, such as
190 *Morchella, Oudemansiella* and *Cortinarius*, also warrant further investigations (17–19).
191 Studying these organisms could provide important insights into the extensiveness of this
192 phenomenon and advance our understanding of chromosome biology and genome evolution.
193 Moreover, the precise molecular mechanisms underlying such chromosome splitting
194 phenomenon remain puzzling and represent an intriguing new area for future research. For
195 instance, how do different nuclei in the same cell communicate and coordinate with each other?
196 What are the key genes and proteins involved in nuclear coordination? Are there special
197 checkpoints to ensure proper chromosomal distribution? Advanced live-cell imaging and single-
198 nuclei sequencing could be particularly valuable for tracking these processes in single cells.

199

200 ## Materials and Methods

201 **Fungal strains and culture conditions**

202 *N. crassa* WT strains 74-OR23-1VA (FGSC#: 2489) and ORS-SL6a (FGSC#: 4200), as well as
203 the hH1-sGFP strains (20) were grown on potato dextrose agar (PDA, Shanghai Bio-way
204 technology, Shanghai, China) and Vogel's minimal media at room temperature under 12 h light/

205 12 h dark conditions (21). Cultures were incubated for approximately 7 days, after which
206 abundant orange conidia were produced and harvested for subsequent experiments.
207 Images of the hH1-sGFP strain were acquired using a 20× objective (NA 0.5) on a ZEISS AXIO
208 Imager M2 microscope. GFP fluorescence was detected using excitation/emission (Ex/Em)
209 wavelengths of approximately 488/509 nm. Scale bars are shown in each image and specified in
210 the figure legends. Brightness adjustments were applied to the images using Zeiss ZEN
211 microscopy software to optimize signal-to-noise and visualize weak signals without altering the
212 original data.
213
214 **Chromosome counting**
215 Conidia of *N. crassa* grown on PDA plates for 10 days were harvested and resuspended in 1.7
216 mL of protoplast buffer (0.8 M $MgSO_4$, 0.2 M sodium citrate, pH 5.5) at a concentration of 10^7
217 spores/mL. Nocodazole was added to a final concentration of 3 μg/mL to arrest the cell cycle.
218 The suspension was incubated with shaking at 28 °C and 200 rpm for 1 hour. Cell wall digestion
219 was then performed by adding 0.3 mL of an enzyme solution (1 M sorbitol, 50 mM sodium
220 citrate, pH 5.8) containing 60 mg of Novozymes VinoTaste Pro, followed by incubation at 28 °C
221 with shaking at 150 rpm for 1 hour.
222 The resulting protoplasts were pelleted by centrifugation at 5000 *g* for 10 minutes, washed once
223 with 2 mL of 0.6 M KCl, and centrifuged again under the same conditions. The pellet was
224 resuspended in 100 μL of 0.6 M KCl and fixed by adding 400 μL of a methanol–acetic acid
225 solution (3:1, v/v). Fixed protoplasts were applied onto glass slides from a height of 10–15 cm
226 and air-dried at room temperature.

227 Slides were stained with DAPI (1 μg/mL) and observed under a ZEISS Axioscope 5 fluorescence
228 microscope with a 100× oil-immersion objective (NA 1.4) for chromosome counting. DAPI
229 fluorescence was detected using Ex/Em wavelengths of approximately 353/465 nm. Upon slide
230 preparation, microscopic examination indicated that fewer than 1% of the protoplasts ruptured,
231 while the majority remained intact with clearly visible nuclei. Due to clustering of some
232 protoplasts, which complicated the assignment of scattered chromosomes, only chromosomes
233 unambiguously contained within a single, ruptured protoplast were included in the analysis.
234 Chromosome numbers were recorded from a total of 105 such ruptured protoplasts and used to
235 construct the chromosome distribution histogram.
236
237 **Monitoring chromosome division in live cells with confocal fluorescence microscopy**
238 Conidia of *N. crassa* (hH1-sGFP strain) were harvested from PDA plates after 7–10 days at room
239 temperature and resuspended in Vogel's medium at a concentration of 10^6 spores/mL.
240 Suspensions were incubated for 3 h at 30°C (225 rpm) to induce germination when active nuclear
241 division begins to occur. Germlings were transferred to 384-well glass-bottom plates (Cellvis)
242 for imaging.
243 Time-lapse imaging was performed on a Leica Stellaris 5 laser-scanning confocal microscope
244 using a 63×/1.40 NA oil-immersion objective. Fields containing cells with 1–5 nuclei were
245 selected (to avoid post-duplication hyphae). GFP was excited at 488 nm and emission collected
246 at 495–530 nm with Tau gating (1–5 ns). Single-plane time series were acquired every 5 or 10 s
247 at 200 Hz scan speed with five-line averaging and a frame size of 512×512 or 1024×512 pixels.
248 Chromosome counts were estimated from condensed chromosome morphology at
249 metaphase/early anaphase. Because chromosomes reorient rapidly during division, counts were

250 refined by examining multiple time points in the series, during which the event presented
251 different orientations; the focal plane was manually adjusted as needed to maintain optimal focus
252 on chromosomes. Image processing and analyses were performed with Fiji (ImageJ, v1.54p).
253
254 **Relative fluorescence intensity (RFI) determination of nuclear DNA content by flow**
255 **cytometry**
256 To measure the DNA content within nuclei, flow cytometry was performed following a previous
257 study with minor modifications, using nuclei isolated from stationary-phase *Saccharomyces*
258 *cerevisiae* liquid cultures and from mycelia of *S. sclerotiorum* and *N. crassa* (1). Briefly, fresh
259 mycelia were collected and grounded into fine powder with liquid nitrogen. Approximately 50
260 mg of the resulting material was resuspended in 2 mL of homogenization buffer [10 mM PIPES
261 (Catalog #AAA1609014; Fisher Scientific), 5 mM CaCl2, 5 mM MgSO4 and 0.5 M sucrose].
262 Samples were centrifuged at 8,000 *g* for 20 minutes at 4°C to pellet nuclei. The nuclei-containing
263 pelleted was resuspended in homogenization buffer and centrifuged at 100 *g* for 5 minutes. Next,
264 1.8 mL of supernatant was transferred to a new tube and centrifuged again at 8,000 *g* for 20
265 minutes. The final pellet, enriched for nuclei, was resuspended in 2 mL of cold sterile 1× PBS
266 buffer (Catalog # B548117; Sangon Biotech).
267 For fluorescence activated cell sorter (FACS) analysis, isolated nuclei were stained with 50
268 µg/mL propidium iodide (PI) for 5-10 minutes. FACS was performed using a Sony MA900
269 Multi-Application cell sorter instrument (Sony Biotechnology, Japan) equipped with a 100 µm
270 sorting chip (LE-C3210), a 488 nm excitation laser, and a 617/30 nm emission detector. Nuclei
271 were gated based on BSC-A (backscatter area) and PI-A (PI fluorescence area) to distinguish
272 populations by size and fluorescence intensity. The sorting was validated by examining sorted

273 nuclei under a fluorescence microscope. Nuclei isolated from S. *cerevisiae*, *S. sclerotiorum* and
274 *N. crassa* mycelia were sorted into 96-well plates, with each species occupying 15 wells and
275 each well containing 100 nuclei. Mean fluorescence intensity values from each well were
276 recorded and used for comparative analysis across samples.
277
278 **FISH analyses**
279 Through BLAST searches of the *N. crassa* genome in FungiDB and EnsemblFungi, a linkage
280 group I (LG I)- specific probe was identified (5' Cy5-
281 CTAGCACCCTTCACTAGCACCCTTCACTAGCACCCTTCA 3'). This specific probe is
282 located at around 7.52 Mb in a non-coding region with a single successive hybridization site,
283 which lies outside of the defined heterochromatin block. In addition, a linkage group IV (LG
284 IV)- specific probe was identified from literature (22), which targets a region around 2.6–2.7 Mb
285 and is not located near sub-telomeric heterochromatic regions (5' Cy5-
286 GTGAACCATCGAGT**Y**TTTGAACGCAAGT 3'). Additionally, a telomere repeat probe
287 capable of targeting all chromosomes and containing multiple adjacent binding sites was
288 identified (5' Cy5- CCCTAACCCTAACCCTAACCCTAACCCTAA 3'). Probes with a 5' Cy5
289 modification were synthesized by Integrated DNA Technologies (IDT).
290 Conidia fixation and FISH were performed following our previous study with minor changes (1).
291 Briefly, the conidia were fixed in an ethanol-acetic acid solution (3:1, v/v) for 3 hours, followed
292 by dehydration through a graded cold ethanol series of 70%, 90%, and 100%, with 5-minute
293 intervals. The samples were then treated with RNase (100 μg/mL in 2× SSC) in a humid
294 chamber at 37°C for 1 hour and subsequently washed four times with 2× SSC at room
295 temperature, with 2-minute intervals. FISH hybridization solution (50% formamide, 10% dextran

296 sulfate, and 2× SSC) was mixed with 100 ng of probe. After adding the hybridization mix, the
297 slides were sealed with a glue gun to prevent evaporation, wrapped in aluminum foil and
298 incubated at 80℃ for 10 minutes to denature genomic DNA. They were then transferred to a
299 moist, dark chamber for hybridization. Hybridization with the nonspecific probe was performed
300 overnight at 37–42 °C, whereas hybridization with the LG I-specific and LG IV-specific probes
301 was carried out for 22 hours at 45 °C and 35–40 °C, respectively. The slides were sequentially
302 washed with 2× SSC at room temperature for 5 minutes, 0.1× SSC at 42–45 °C for 10 minutes,
303 and 2× SSC at room temperature 5 minutes, followed by dehydration through the cold ethanol
304 series. Prior to imaging, 20 µl of 1 µg/mL DAPI (Sigma-Aldrich, Canada) was added to stain
305 nuclei. 5 µl of VECTASHIELD HardSet Antifade Mounting Medium (Vector Labs, USA) was
306 applied, and the slide was sealed with clear nail polish (Sally Hansen 109 invisible, Canada) to
307 preserve fluorescence. The cells without signals inside the nuclei are considered samples failed
308 the experiment (column "Number of conidia without signals inside the nuclei").
309 Images of FISH samples were acquired using a 100× oil-immersion objective (NA 1.4) on a
310 ZEISS AXIO Imager M2 microscope. DAPI (Ex/Em ≈ 353/465) and Cy5 (Ex/Em ≈ 650/673)
311 fluorescence were used. Scale bars are shown in each image and specified in the figure legends.
312 Brightness adjustments were applied to the images using Zeiss ZEN microscopy software to
313 optimize signal-to-noise and visualize weak signals without altering the original data.
314

315 **Acknowledgments**

316 We thank Josh Li for assistance *N. crassa* conidia cultivation, and Dr. Lei Tian and Xuanye
317 Chen for careful reading of the manuscript. We are grateful to Prof. Yi Yang (SU) for sharing
318 their ZEISS fluorescence microscope for chromosome counting. ChatGPT 5.0 (OpenAI, San

Francisco, CA, USA) was used for correcting grammar mistakes and language polishing. This work was supported by funds to Y.X. from National Key Research and Development Program of China (2025YFF1000600) and to X.L. from the Canadian Natural Sciences and Engineering Research Council (NSERC) Discovery program, NSERC-CREATE-PRoTECT, Canada Research Chair (CRC), and the Canadian Foundation for Innovation (CFI) funds. J.T. is partly supported by a UBC Four-year Fellowship.

Reference

1. Xu Y, Tian L, Tan J, Huang W, Li J, O'Neil N, et al. Distribution of haploid chromosomes into separate nuclei in two pathogenic fungi. Science. 2025;388(6748):784–788. https://doi.org/10.1126/science.abn7811
2. Fukumori Y, Nakajima M, Akutsu K. Microconidia act the role as spermatia in the sexual reproduction of *Botrytis cinerea*. J Gen Plant Pathol. 2004;70:256–60. https://doi.org/10.1007/s10327-004-0124-9
3. Wong JAL, Willetts HJ. Cytology of *Sclerotinia sclerotiorum* and related species. Microbiology. 1979;112:29–34. https://doi.org/10.1099/00221287-112-1-29
4. Tian L, Chen X, Weerasinghe T, Wang A, Wang S, Zhang Y, et al. Beyond the "One Nucleus, One Whole Genome" rule. Trends in Genetics. 2026; 42(3):212-214. https://doi.org/10.1016/j.tig.2026.01.001
5. Pandit A, Maheshwari R. A simple method of obtaining pure microconidia in *Neurospora crassa*. Fungal Genetics Reports. 1993;40:24.
6. Maheshwari R. Microconidia of *Neurospora crassa*. Fungal Genetic and Biology. 1999;26:1–18. https://doi.org/10.1006/fgbi.1998.1103
7. Davis RH, Perkins DD. Neurospora: A model of model microbes. Nature Review Genetics. 2002;3(5):397–403. https://doi.org/10.1038/nrg797
8. Beadle GW, Tatum EL. Neurospora. II. Methods of producing and detecting mutations concerned with nutritional requirements. American Journal of Botany. 1945;32(10):678–686. https://doi.org/10.2307/2437625
9. Schulte U, Becker I, Mewes HW, Mannhaupt G. Large scale analysis of sequences from *Neurospora crassa*. Journal of Biotechnology. 2002;94(1):3–13. https://doi.org/10.1016/S0168-1656(01)00415-1
10. Galagan JE, Calvo SE, Borkovich KA, Selker EU, Read NO, Jaffe D, et al. The genome sequence of the filamentous fungus *Neurospora crassa*. Nature. 2003;422(6934):859–868. https://doi.org/10.1038/nature01554
11. Wu VW, Thieme N, Huberman LB, Dietschmann A, Kowbel DJ, Lee J, et al. The regulatory and transcriptional landscape associated with carbon utilization in a filamentous fungus. Proceedings of the

351 National Academy of Sciences of the United States of America. 2020;117(11):6003–6013.
352 https://doi.org/10.1073/pnas.1915611117
353 12. Orbach MJ, Vollrath D, Davis RW, Yanofsky C. An electrophoretic karyotype of *Neurospora crassa.*
354 Molecular and Cellular Biology.1 988;8(4), 1469–1473. https://doi.org/10.1128/mcb.8.4.1469-1473.1988
355 13. Colot H V., Park G, Collopy PD, Krystofova S, Ringelberg C, Crew C, et al. How to create gene knockouts
356 in Neurospora [Internet]. Fungal Genetics Stock Center. 2007. Available from:
357 https://www.fgsc.net/neurosporaprotocols/How to create gene knockouts in Neurospora.pdf
358 14. Case M. How to use UV for mutagenesis [Internet]. Fungal Genetics Stock Center. 2007. Available from:
359 https://www.fgsc.net/neurosporaprotocols/How to use UV for mutagenesis.pdf
360 15. Xu Y, Ao K, Tian L, Qiu Y, Huang X, Liu X, et al. A forward genetic screen in *Sclerotinia sclerotiorum*
361 revealed the transcriptional regulation of its sclerotial melanization pathway. Molecular Plant-Microbe
362 Interaction. 2022; 35(3):244–256. https://doi.org/10.1094/MPMI-10-21-0254-R
363 16. Schmit JC, Brody S. Biochemical genetics of *Neurospora crassa* conidial germination. Bacteriological
364 Review. 1976;40(1):1–41. https://doi.org/10.1128/mmbr.40.1.1-41.1976
365 17. Horton TR. The number of nuclei in basidiospores of 63 species of ectomycorrhizal Homobasidiomycetes.
366 Mycologia. 2006;98(2):233–238. https://doi.org/10.1080/15572536.2006.11832695
367 18. Rebecca R, Gao Q, Cui Y, Rong C, Liu Y, Zhao W, et al. Nuclear conditions of basidiospores and hyphal
368 cells in the edible mushroom *Oudemansiella aparlosarca*. Microbiologyopen. 2021;10(5):e1233.
369 https://doi.org/10.1002/mbo3.1233
370 19. Du XH, Wang SY, Ryberg M, Guo YJ, Wei JY, Pfister DH, et al. Cytological studies reveal high variation
371 in ascospore number and shape and conidia produced directly from ascospores in *Morchella galilaea*.
372 Frontiers in Microbiology. 2023;14: 1–20. https://doi.org/10.3389/fmicb.2023.1286501
373 20. Freitag M, Hickey PC, Raju NB, Selker EU, Read ND. GFP as a tool to analyze the organization , dynamics
374 and function of nuclei and microtubules in *Neurospora crassa*. Fungal Genetetic and Biology.
375 2004;41(10):897–910. doi: 10.1016/j.fgb.2004.06.008
376 21. Vogel HJ. A Convenient Growth Medium for *Neurospora crassa*. Microbial Genetics Bulletin. 1956;13:42–
377 7.
378 22. Waminal NE, Pellerin RJ, Kim NS, Jayakodi M, Park JY, Yang TJ, et al. Rapid and efficient fish using pre-
379 labeled oligomer probes. Scientific Report. 2018;8(1):1–10. https://doi.org/10.1038/s41598-018-26667-z
380
381
382
383

384 ## Supporting information

385 **S1 Movie. Live chromosome division in *N. crassa* conidia.**

386 Germinating conidia expressing hH1–sGFP were imaged by laser-scanning confocal microscopy
387 at room temperature. Frames highlight anaphase segregation with an estimated two
388 chromosomes visible. Scale bar, 2 μm. The GFP channel is shown in (A), and the merged
389 channel is shown in (B).

390

391 **S2 Movie. Live chromosome division in *N. crassa* young mycelia.**

392 A young mycelium tip germinated from a conidium expressing hH1–sGFP was imaged by laser-
393 scanning confocal microscopy at room temperature. Frames highlight prophase condensation,
394 with an estimated number of four chromosomes visible. Scale bar, 2 μm. The GFP channel is
395 shown in (A), and the merged channel is shown in (B).

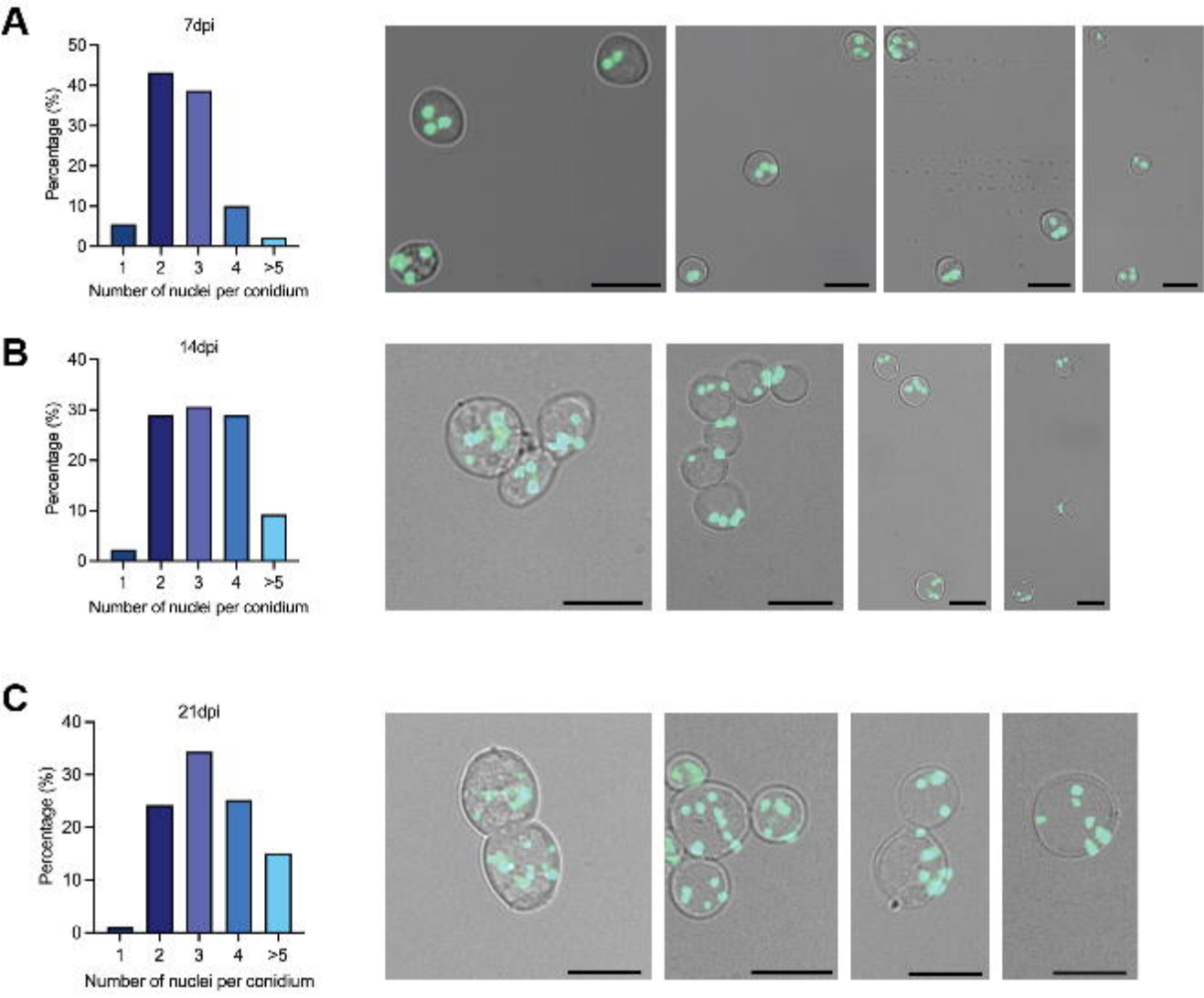
A
7dpi
Percentage (%)
50
40
30
20
10
0
1
2
3
4
>5
Number of nuclei per conidium
B
14dpi
Percentage (%)
40
30
20
10
0
1
2
3
4
>5
Number of nuclei per conidium
C
21dpi
Percentage (%)
40
30
20
10
0
1
2
3
4
>5
Number of nuclei per conidium

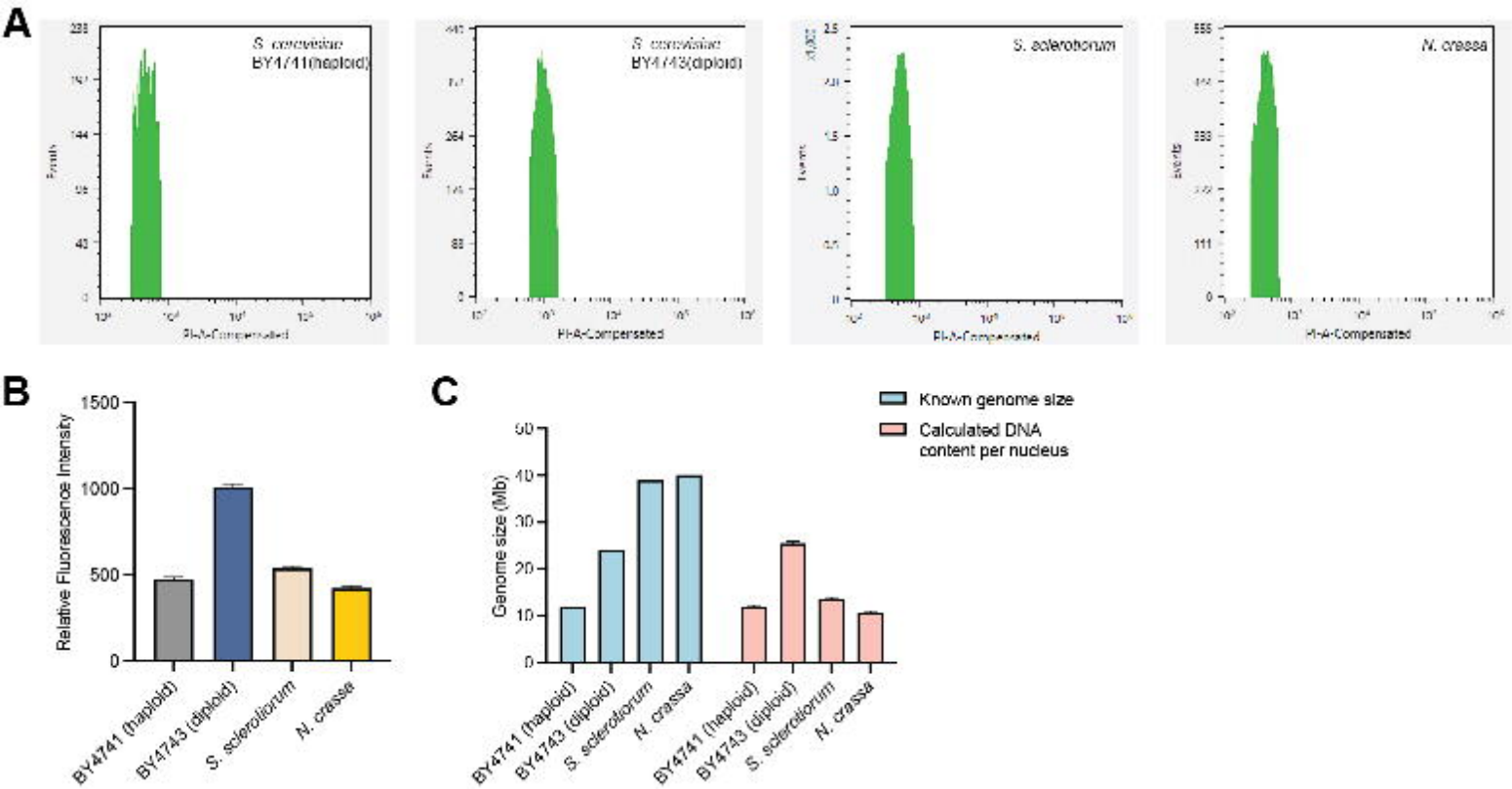
A
S. cerevisiae
BY4741(haploid)
S. cerevisiae
BY4743(diploid)
S. sclerotiorum
N. crassa
Events
PI-A-Compensated
B
Relative Fluorescence Intensity
1500
1000
500
0
BY4741 (haploid)
BY4743 (diploid)
S. sclerotiorum
N. crassa
C
Known genome size
Calculated DNA content per nucleus
Genome size (Mb)
50
40
30
20
10
0
BY4741 (haploid)
BY4743 (diploid)
S. sclerotiorum
N. crassa
BY4741 (haploid)
BY4743 (diploid)
S. sclerotiorum
N. crassa

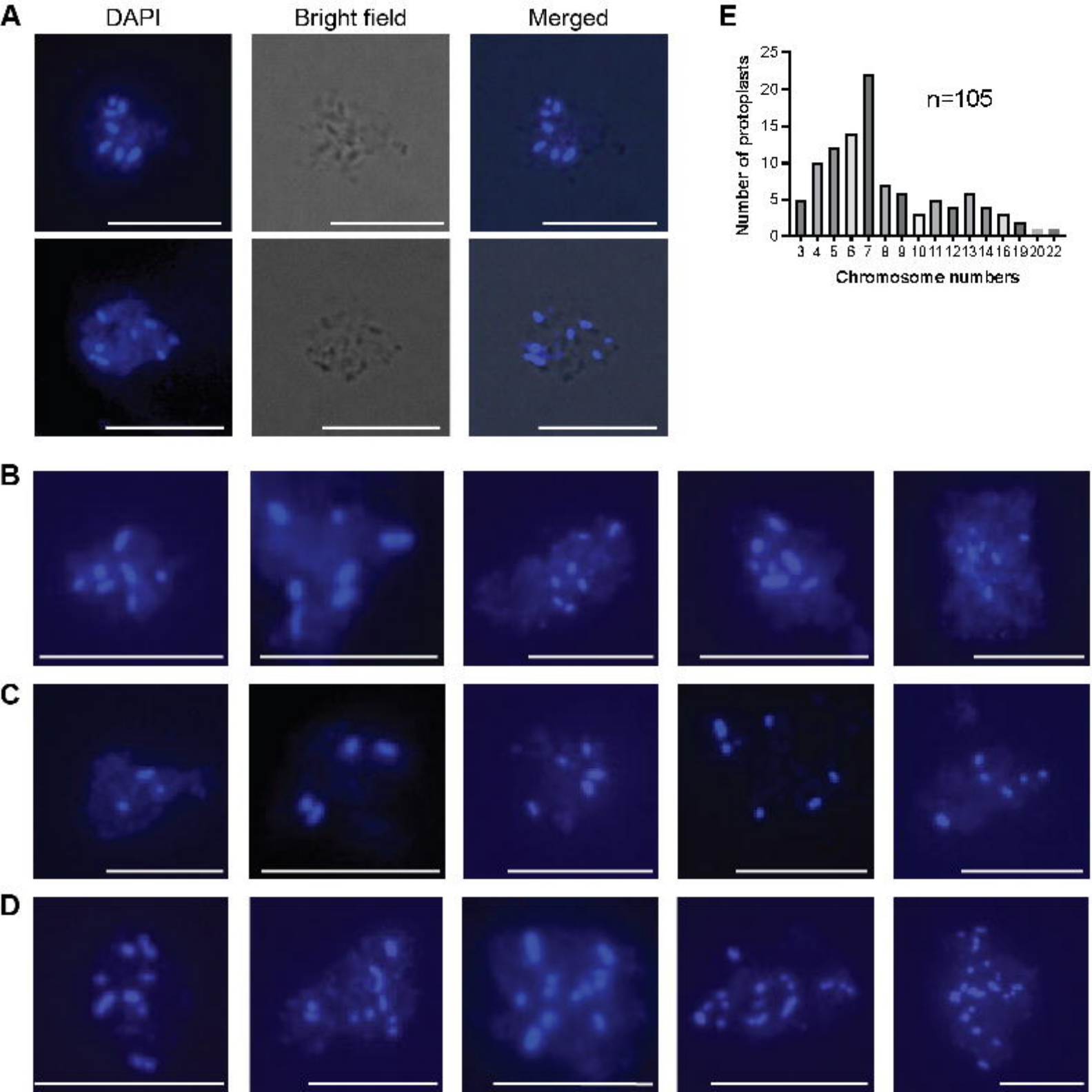
A
DAPI
Bright field
Merged
E
n=105
Number of protoplasts
Chromosome numbers
B
C
D

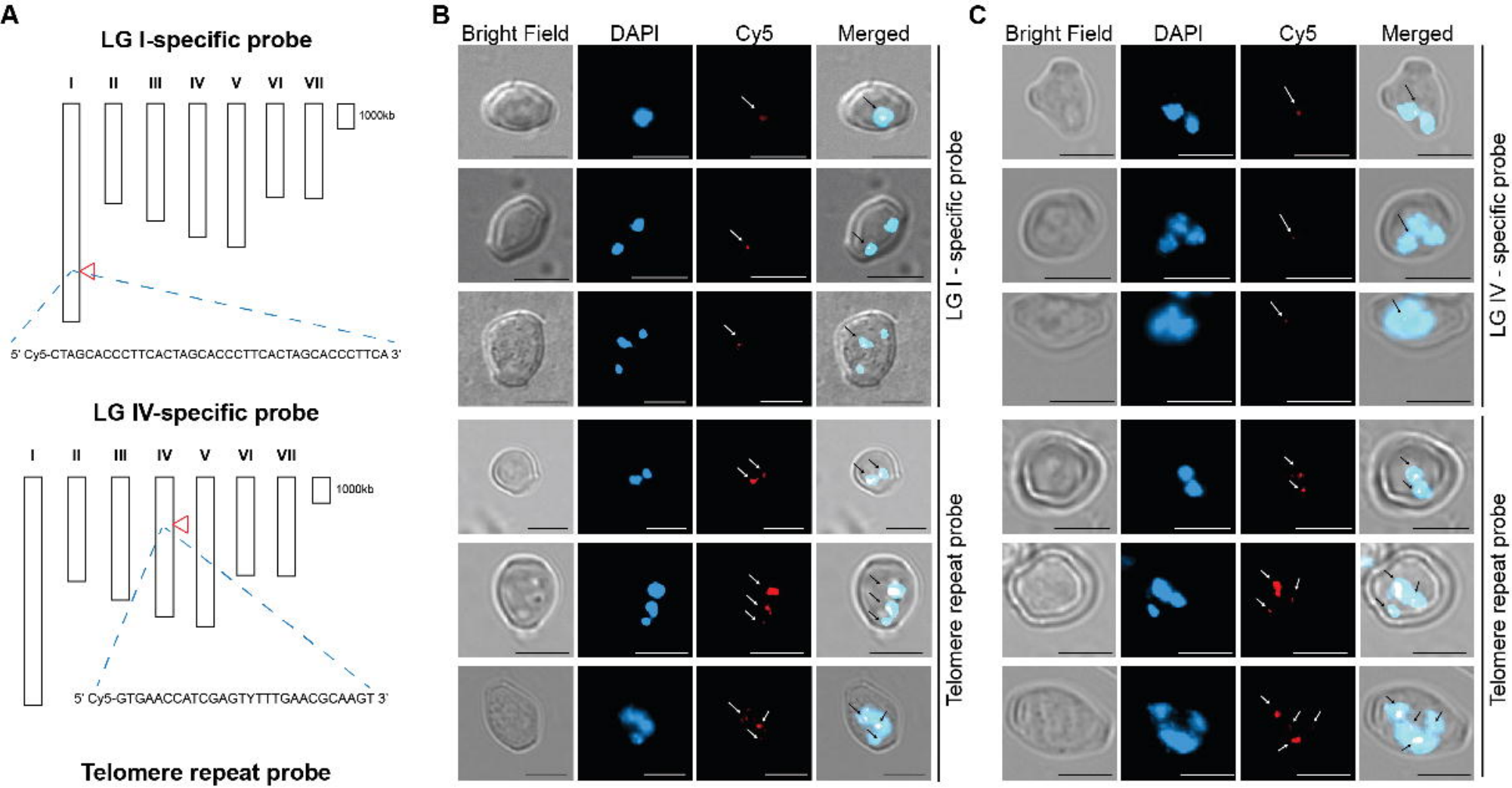

D

Probe	No. of conidia without probe signal inside any nucleus	No. of conidia with probe signal in one nucleus	No. of conidia with probe signals in two or more nuclei	Total numbers of conidia
LG I -specific probe	23	171	0	194
LG IV -specific probe	108	22	0	130

Probe	No. of conidia without probe signal inside any nucleus	No. of conidia with probe signals in over half of nuclei	No. of conidia with probe signals in all nuclei	Total numbers of conidia
Telomere repeat probe	15	29	79	123